analytical chemistry

pubs.acs.org/ac Article

Ultrahigh Resolution Ion Isolation by Stored Waveform Inverse Fourier Transform 21 T Fourier Transform Ion Cyclotron Resonance Mass Spectrometry

Donald F. Smith, Greg T. Blakney, Steven C. Beu, Lissa C. Anderson, Chad R. Weisbrod, and Christopher L. Hendrickson*

Cite This: *Anal. Chem.* 2020, 92, 3213−3219 Read Online

ACCESS | Metrics & More | Article Recommendations | Supporting Information

ABSTRACT: Stored waveform inverse Fourier transform (SWIFT) is a versatile method to generate complex isolation/ejection waveforms for precursor isolation prior to tandem mass spectrometry experiments. Here, we report ultrahigh resolving power ion isolation by SWIFT on a 21 T Fourier transform ion cyclotron resonance (FTICR) mass spectrometer. Individual histone proteoforms are isolated (0.6 m/z isolation window) with near 100% efficiency using a 52 ms SWIFT isolation, followed by in-cell fragmentation by ultraviolet photodissociation (UVPD). Ion isolation resolving power of 175 000 ($m/\Delta m$) is demonstrated by isolation of individual peaks at a spacing of 0.0034 Da at m/z 597 from a complex mixture of Canadian bitumen. An individual m/z ion, which corresponds to a single elemental composition, from a complex mixture is isolated and fragmented by infrared multiphoton dissociation (IRMPD). Theoretical and experimental considerations that limit achievable ion isolation resolving power are discussed.

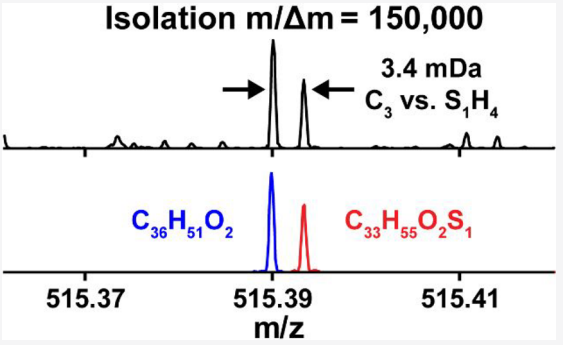

High-quality tandem mass spectrometry relies on the resolution and efficiency of ion isolation prior to fragmentation. Selectivity in the ion isolation step is paramount for the analysis of highly complex samples, such as proteins by top-down mass spectrometry[1−3] and complex organic mixtures (e.g., petroleum and dissolved organic matter).[4−6] Most tandem mass spectrometers isolate precursor ions by ion trap devices or mass selective quadrupoles, which have low ion isolation resolving power, typically <1 000. Co-isolation of unwanted precursor ions can complicate tandem mass spectra interpretation, result in poorly scored tandem mass spectra due to coisolated contaminants within the isolation window, or even misidentification of the analyte entirely.[7] In addition, contaminants or unwanted coisolated species can limit the utility of automatic gain control (AGC) based ion accumulation and limit observed dynamic range within the resultant spectrum.

Fourier transform ion cyclotron resonance mass spectrometry (FTICR MS) has traditionally offered the highest resolution ion isolation capability of any mass analyzer. In addition, ion isolation resolving power improves linearly with magnetic field strength, such that modern, high magnetic field FTICR systems offer isolation resolving powers >20 000. Single frequency excitation and ejection of selected ions has achieved an isolation resolving power of 50 000 at m/z 79.[8] This method was shown to be hampered by unavoidable off-resonance excitation of ions that were selected for isolation. The correlated harmonic excitation field (CHEF) isolation method has also achieved an isolation resolving power of 50 000 at m/z 80,[9] and has been used to isolate single protein isotopologues with an isolation resolving power of 17 000 at m/z 808.[13] Stored waveform inverse Fourier transform (SWIFT)[10−12] has also been used to isolate single protein isotopologues, with an isolation resolving power of 29 000 at m/z 969.[14] SWIFT technology has also been applied to ion trap mass spectrometers for excitation and ion isolation.[15,16]

Phase-enhanced selective ion ejection has been used in an Orbitrap Fourier transform mass spectrometer (FTMS) to achieve an isolation resolving power of 28 400 at m/z 516.[17] However, the Orbitrap instrument configuration does not allow fragmentation of precursors isolated in the Orbitrap analyzer, which limits the analytical utility of such experiments. In addition, application of resonant dipolar ac waveforms to the outer detection electrodes of an Orbitrap is not currently commercially available. Multireflectron-time-of-flight (MR-TOF) mass spectrometers can achieve high ion isolation resolving powers due to their long path length. Recently, MR-TOF instruments have achieved ion isolation resolving powers

Received: October 30, 2019
Accepted: January 21, 2020
Published: February 3, 2020

https://dx.doi.org/10.1021/acs.analchem.9b04954
Anal. Chem. 2020, 92, 3213−3219

of 40 000 by square wave modulation,[18] and up to 70 000 by selective retrapping.[19] Similarly, an electrostatic linear ion trap was recently shown to achieve an isolation resolving power of ~60 000 with mirror switching.[20]

As commercial mass spectrometer performance has improved, the complexity of mixtures that can be analyzed has increased. Accordingly, ion isolation for tandem MS experiments should complement the high mass resolving power in the precursor scan. For top-down proteomics, however, isolation of precursors is typically performed with a 5−15 m/z window for hybrid ion trap-FTMS systems[21,22] and ~3 m/z for quadrupole-FTMS systems.[23] This is due mainly to loss of isolation efficiency at more narrow isolation widths. Recently, Zheng et al. reported quadrupole isolation widths of 0.6 m/z for histone H3 proteoform characterization on an Orbitrap Fusion Lumos mass spectrometer.[24] Additionally, Guan and Burlingame modified a commercial hybrid ion trap FTICR MS to enable SWIFT ion isolations of ~1 m/z for direct infusion experiments to characterize histone H4 by electron capture dissociation.[25]

Organic mixtures from petroleum constitute some of the most complex mixtures in the world. Ultrahigh mass resolving power FTICR MS is ideal for molecular characterization of these mixtures, where tens of thousands of unique elemental compositions are resolved and assigned with high mass measurement accuracy. However, structural characterization of these mixtures by tandem mass spectrometry is difficult due to the large number of individual components; for example, atmospheric pressure photoionization (APPI) of an asphalt volcano sample shows 462 peaks in a single nominal mass at m/z 677.[6] Tandem mass spectrometry of 1 m/z isolation windows has been performed; however, the isolation window is still too wide to ensure multiple precursors are not coisolated and fragmented.[26,27] Detailed structural characterization of subnominal mass units is desirable, to further limit the compositional space being fragmented, with the ultimate goal of high-resolution isolation of only a single m/z species from such complex mixtures.[28]

In this manuscript, we describe the advantages of SWIFT for high resolving power ion isolation on a 21 T FTICR mass spectrometer. Histone proteoforms separated by liquid chromatography (LC) are isolated with greater than 80% efficiency with an isolation width of 0.6 m/z in 52 ms, followed by detailed top-down tandem MS by ultraviolet photodissociation (UVPD). Ion isolation resolving power of 175 000 is demonstrated on a complex organic mixture. Finally, a single m/z species from a complex mixture is isolated and fragmented by infrared multiphoton dissociation (IRMPD).

EXPERIMENTAL METHODS

Mass Spectrometry. Experiments were performed on a custom-built 21 T hybrid ion-trap FTICR mass spectrometer described previously.[6,22,29] The dynamically harmonized ICR cell (DHC)[30] is segmented into 12 biconcave and 12 biconvex electrodes, and excitation and detection are performed on 120° cell segments for improved excitation electric field, detection sensitivity, and minimization of third harmonic signals.[29,31,32] The improvement in excitation electric field uniformity and minimization of postexcitation ion cloud expansion for the 120° excitation geometry should improve SWIFT isolation performance.[33] SWIFT waveform generation, application, ion excitation, and ion detection were performed with the Predator data acquisition system.[34] Predator uses a National Instruments PXIe-5442 arbitrary waveform generator for excitation waveforms, with a 43 MHz bandwidth and onboard memory depth of 16 million samples. All SWIFT waveforms used a smoothing filter width of three,[35] a quadratic phase function,[12,35,36] and a sampling rate of 2×10^7 samples/second (10 MHz Nyquist frequency) to ensure accurate waveform fidelity over the excited bandwidth (20 kHz−2.5 MHz). Single-frequency excitation experiments used an excitation duration of 300 μs, and the excitation amplitude was increased from ~66 to 200 $V_{p\text{-}p}$, which corresponds to a percent cell radius of ~32−98%.[37]

A barium fluoride window is mounted on the ICR cell flange which enables both UVPD (λ = 193 nm) and IRMPD (λ = 10.6 μm) to be performed. UVPD was performed with a 193 nm argon fluoride excimer laser (ExciStar XS 500; Coherent, Santa Clara, CA). A 30 W Firestar CO_2 laser (Synrad, Inc., Mukilteo, WA) was focused into the ICR cell with a ZnSe plano-convex lens (f = 1000 mm; Thorlabs, Newton, NJ) for IRMPD.

Bitumen. Athabascan Canadian bitumen was diluted to a final concentration of 250 μg/mL in 50:50 methanol/toluene with 0.125% (v/v) TMAH solution added to aid deprotonation for electrospray ionization (ESI). A 5 m/z ion trap isolation (2 fills with an AGC target of 5×10^4 charges each, 1×10^5 charges total) was performed prior to ion transfer to the ICR cell. SWIFT isolation waveforms of 16 or 32 MB were used for high-resolution ion isolation and 10 spectra were coadded (~4.2 s per scan for 16 MB, ~5 s per scan for 32 MB).

A final concentration of 50 μg/mL in toluene was used for atmospheric pressure photoionization (APPI). An initial ion trap isolation of 3.5 m/z (AGC target of 3×10^6 charges) was performed prior to high-resolution SWIFT isolation of a single m/z value (16 MB waveform) and IRMPD (22.5 W), and 60 spectra were coadded (~6.2 s per scan). Peaks with a signal magnitude greater than 6 times the baseline root-mean-square (rms) noise at m/z 352 were exported to a peak list and molecular formula assignments and data visualization were performed with PetroOrg software (v18.0.5; Florida State University, Tallahassee, FL).[38] All bitumen experiments used a detection duration of 3.2 s, which yields a magnitude mode mass resolving power of 1 290 000 at m/z 400.

Histones. Histones isolated from *Drosophila melagonaster* (~2 pmol of total protein) were loaded onto an in-house-fabricated 360 μm o.d. x 150 μm i.d. fused-silica microcapillary trap column packed 2.5 cm with Poroshell C8 resin (5 μm particle, 300 Å pore, Agilent Technologies, Palo Alto, CA). The LC system (Acquity M-Class, Waters, Milford, MA) was operated at a flow rate of 2.5 μL/min for loading onto the trap column and washed with 95% solvent A for 10 min. Separation was achieved on an in-house-fabricated analytical column packed 17.5 cm with Poroshell C8 resin. Samples were gradient eluted at a flow rate of 0.3 μL/min over 60 min. The gradients utilized solvent A, 0.3% formic acid and 5% acetonitrile in water, and solvent B, 47.5% acetonitrile, 47.5% 2-propanol, 4.7% water, and 0.3% formic acid (% all expressed as v/v). Following separation, proteins were directly ionized by nanoelectrospray ionization (2.5−3.0 kV source voltage) using a 15 μm fused-silica PicoTip emitter (New Objective, Woburn, MA) packed with ~3 mm of PLRP-S (poly(styrene-*co*-divinylbenzene)) resin. The instrument was operated in targeted mode. Precursors were selected as they eluted from

https://dx.doi.org/10.1021/acs.analchem.9b04954
Anal. Chem. 2020, 92, 3213−3219

the column and isolated in the ion trap with a 10 m/z isolation width (cumulative AGC ion target of 2×10^7 charges) prior to ion transfer to the ICR cell. Histone isoforms were isolated with 0.6 m/z SWIFT waveforms (1 M, 52.4 ms), followed by a single UV laser pulse (1.6 mJ). The detection duration was 398 ms, which yields a magnitude mode mass resolving power of 160 000 at m/z 400 (scan time ~1−1.5 s). The THRASH algorithm was used for peak deconvolution (minimum signal-to-noise ratio, 3.0; match parameter, 0.85),[39] and fragments were matched to putative sequences with ProSight Lite (v1.4, build 1.4.6; Northwestern University, Evanston, IL) with UVPD set as the fragmentation method and a fragment tolerance of ±10 ppm.[40]

RESULTS AND DISCUSSION

SWIFT Waveform Construction, Considerations, and Limitations. SWIFT waveforms for high-resolution ion isolation are constructed as depicted in Figure 1. First, the m/z range for isolation is identified, where a notch with zero excitation amplitude is defined and where maximum excitation amplitude is applied to the remainder of the m/z range (Figure 1a). The instrument calibration equation is used to convert from m/z to frequency domain (Figure 1b). Inverse Fourier transform of the smoothed frequency domain waveform (with a quadratic phase function) yields the time-domain excitation waveform, which is downloaded to the arbitrary waveform generator (AWG) of the data station (Figure 1c). The AWG applies the waveform to the excitation electrodes in the ICR cell, selectively ejecting the unwanted ions, and subsequent excitation and detection yields a mass spectrum of the m/z range of interest. Waveforms can be created with user-defined parameters, selected from a library of predefined waveforms, or generated from data-dependent selection criteria.

The duration of the ion isolation event and the bandwidth, i.e., the waveform size, determine the maximum achievable isolation resolving power for SWIFT, whereas mass resolving power for ion detection is determined by the duration of the time-domain detection event. Figure 2 shows the frequency domain of different sizes of the same SWIFT waveform; the defined notch width is 8 Hz centered at a frequency of 626.77675 kHz. A waveform of 8 MB is insufficient to define the desired isolation, with only a small portion of the waveform amplitude at zero. The slopes of the notch edges increase with increased waveform size, as does the width of the near-zero amplitude portion of the waveform.

Excitation electronics will affect the fidelity of the applied SWIFT waveform, which can result in lower than expected isolation resolving power. The excitation amplification circuit, waveform phase and amplitude balance, and nonuniform excitation amplitude will cause deviations from the expected theoretical isolation resolving power. Figure S-1a shows the optimized 16 MB time domain SWIFT waveform discussed in Figure 2, and Figure S-1b shows the waveform measured after the excitation electronics, where nonuniform excitation amplitude is visible. The frequency domain SWIFT waveform (no apodization, two zero-fills) is shown in Figure S-2. The optimized SWIFT waveform is shown in red, and the measured waveform is shown in blue. Figure S-2a shows the full bandwidth of the SWIFT excitation, where nonuniform excitation amplitude is visible. Figure S-2b shows a frequency domain expanded inset of the isolation notch, where the applied waveform notch edges have a lower slope than the optimized waveform, the center of the notch is shifted slightly

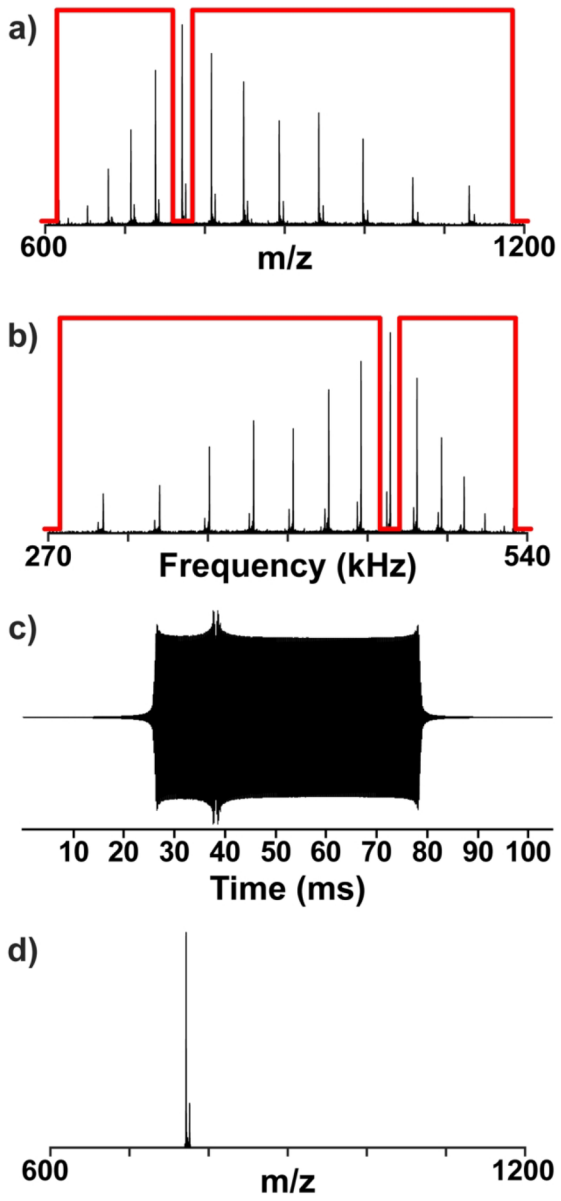

Figure 1. Illustration of SWIFT isolation by FTICR MS: (a) create notch in the m/z domain, (b) convert to the frequency domain, (c) inverse Fourier transform of the smoothed frequency domain (with quadratic phase function) yields the time domain waveform. (d) Waveform is applied to excitation cell electrodes; ions in the notch are retained, and ions outside the notch are ejected from the ICR cell.

(~1 Hz) in frequency, and deviations from the desired waveform amplitude are visible. These deviations from the optimized waveform will all affect the maximum achievable isolation resolution.

In addition, the cyclotron frequencies of ions will change over the course of the SWIFT isolation event as the cyclotron radius changes. Magnetic field homogeneity and electric field harmonization effect how much the cyclotron frequency will change. Thus, the width of the isolation notch cannot be less than this frequency drift, otherwise the ions can move out of the isolation notch during the SWIFT event. The National High Magnetic Field Laboratory (NHMFL) 21 T magnet has spatial inhomogeneity of less than 5 parts-per-million (ppm) over a 60 mm × 100 mm cylindrical volume, which is the approximate working volume of the NHMFL DHC (56 mm

https://dx.doi.org/10.1021/acs.analchem.9b04954
Anal. Chem. 2020, 92, 3213−3219

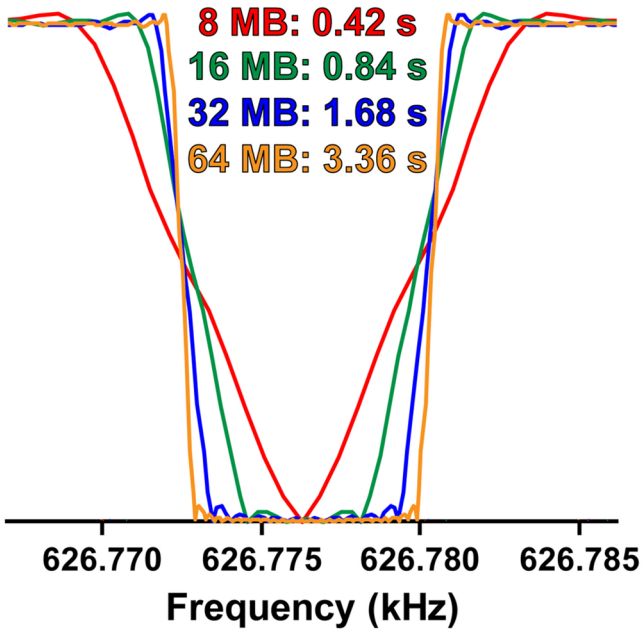

Figure 2. SWIFT waveform size (length) determines maximum achievable ion isolation resolving power. Larger waveforms have sharper edges, and the width of the zero amplitude portion of the notch is larger. The width of the notch is kept constant at 8 Hz.

inner diameter, 145.7 mm length). Thus, frequency shifts due to inhomogeneous magnetic field strength are minimized. The DHC approximates a hyperbolic trapping electric field, via potential averaging over the cyclotron orbit, thus minimizing frequency shifts due to the distribution of ion z-axis kinetic energy. Figure 3 shows the frequency change versus percent cell radius of two ions from (−) ESI of Athabascan Canadian bitumen from a single-frequency excitation experiment. The two ions (m/z 515.38938 and 515.39275), differ in m/z by 3.4 mDa or 4.1 Hz. Both ions have a cyclotron frequency shift of less than 1 Hz (∼1 ppm) over the accessible excitation volume

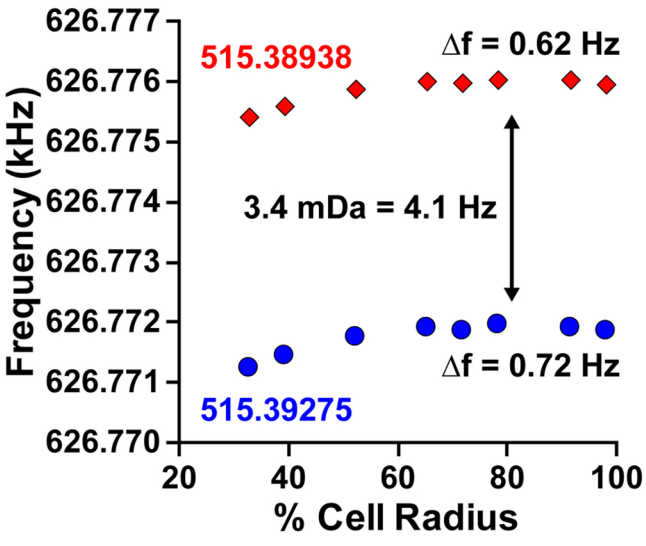

Figure 3. Cyclotron frequency as a function of percent cell radius for single frequency excitation of two ions that differ in m/z by 3.4 mDa or 4.1 Hz (m/z 515.38938 and 515.39275) from (−) ESI of Athabasca Canadian bitumen. The change in cyclotron frequency is less than 1 Hz over the radius of the ICR cell.

of the DHC. Thus, the minimum isolation notch width for isolation of either of these two ions would be ∼1 Hz.

Rapid, High-Selectivity SWIFT Isolation of Histone Proteoforms. The 21 T enables rapid SWIFT isolation of proteoforms from complex protein mixtures, since the time required for a desired isolation resolving power is inversely proportional to magnetic field strength. Histones from *Drosophila melagonaster* were chosen to illustrate the utility of SWIFT for analysis of complex proteoform mixtures. Histones are multimeric protein complexes which are heavily modified in a diverse combinatory manor responsible for the exposure of certain genes for transcription and the packaging of DNA into nucleosomes. This modification "code" has been a focal point for science since its discovery, perhaps due to its epigenetic character and that these modification states have been shown to be heritably passed from parent to progeny. Histones can have extensive post-translation modifications, which yield complex mass spectra. Fast, efficient, and selective isolation of proteoforms is key for high-quality tandem mass spectrometry to determine modification sites. Figure 4a shows

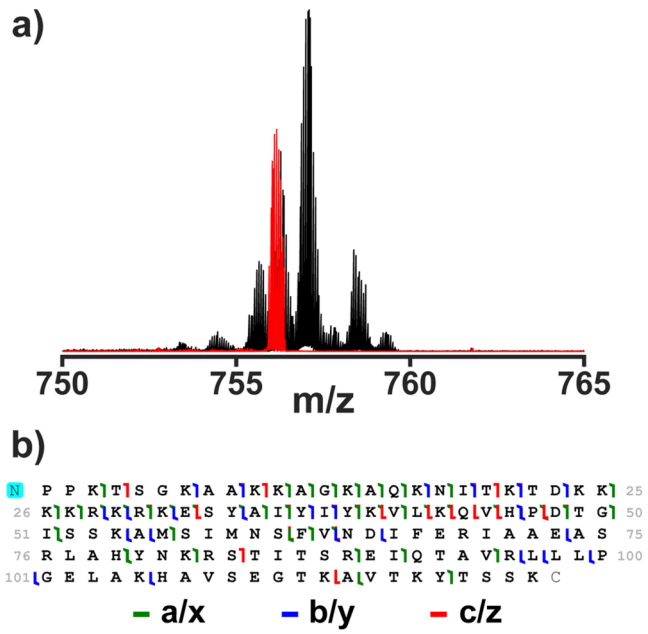

Figure 4. SWIFT isolation of histone H2B from LC−MS of bulk histones. (a) Black trace: initial 10 m/z ion trap isolation with at least eight coeluting proteoforms. Red trace: SWIFT isolated H2B proteoform. (b) Sequence coverage map from single pulse UVPD from ProSightLite. The sequence coverage is 53%, with an N-terminal demethylation. All spectra are the summation of 20 transients.

a mass scale expanded segment from an liquid chromatography−tandem mass spectrometry (LC−MS/MS) analysis of histone proteoforms from*Drosophila melagonaster*. At least eight proteoforms are coisolated in the initial 10 m/z ion trap isolation (shown in black). A SWIFT isolation of 0.6 m/z cleanly isolates the H2B proteoform shown in red, with near 100% efficiency in only 52.5 ms. Here, isolation efficiency is defined as the percent difference in signal magnitude between the initial ion trap isolation spectrum and post-SWIFT isolation spectrum. The subsequent UVPD, with a single laser pulse, results in the fragmentation map shown in Figure 4b, with 53% coverage of all possible residue cleavages and identifies a demethylation on the N-terminus. The spectrum is

https://dx.doi.org/10.1021/acs.analchem.9b04954
Anal. Chem. 2020, 92, 3213−3219

a sum of 20 transients that eluted over the course of ~1.3 min. Supporting Information Figures S-3 and S-4 show two additional examples of detailed online proteoform characterization with this method.

Here, large ion populations (2×10^7 charges) are initially isolated in the ion trap with a large isolation window. This avoids ion trap space charge limitations for isolation and ensures high signal-to-noise for UVPD tandem MS experiments. Further, minimal precursor ion fragmentation is observed upon SWIFT isolation, where neutral loss fragments are detected with relative abundance less than 0.5% (data not shown).

Ultrahigh Isolation Resolving Power SWIFT. A sample of Athabascan Canadian bitumen was used to assess the ultrahigh ion isolation capabilities of the 21 T FTICR MS. A mass difference of 3.4 mDa (C_3 versus S_1H_4) is prevalent across the m/z range in petroleum samples, which is used here to test the limits of ion isolation (see Figure S-5 for the broadband mass spectrum). Figure 5a (top) shows a mass scale expanded segment of the initial 5 m/z ion trap isolation at m/z 515 and SWIFT isolation of each m/z comprising the 3.4 mDa mass difference (middle, bottom). An isolation efficiency of ~50% was achieved, and an isolation resolving power of 150 000 is required to isolate ions that differ by 3.4 mDa at m/z 515. The SWIFT waveform was 16 MB (0.84 s), and 10 spectra were coadded for each experiment. Figure 5b (top) shows a mass scale expanded segment of the initial 5 m/z ion trap isolation at m/z 597 and SWIFT isolation of each m/z comprising the 3.4 mDa mass difference (middle, bottom). A 16 MB waveform could not cleanly isolate either of these species, so a 32 MB SWIFT (1.68 s) waveform was used. The isolation resolving power required is 175 000, which is achieved with an efficiency of ~17%, as shown in Figure 5b (middle, bottom). The decreased isolation efficiency suggests deviation from the theoretical SWIFT waveform as discussed above or loss of ions due to collisional damping in the ICR cell. Nevertheless, these experiments illustrate the highest isolation resolving power achieved by mass spectrometry to date.

Isolation and Tandem Mass Spectrometry of SWIFT Isolated Unique *m/z* Ions. FTICR MS is the method of choice for the characterization of complex organic mixtures, where molecular formulas of detected ions ($C_cH_hN_nO_oS_s$) are assigned with low mass measurement error (<1 ppm). However, the compositional complexity hampers tandem mass spectrometry for structural characterization, as multiple precursor ions are typically coisolated prior to tandem MS analysis. The methods described herein now enable single precursor ion selection from complex organic mixtures to mass differences as small as 3.4 mDa.

A sample of Athabascan Canadian bitumen was analyzed by (+) APPI with an initial ion trap isolation of 3.5 m/z. There are 210 peaks at nominal mass 352 (6σ peak picking level), and the precursor ion is 3.4 mDa from the next abundant ion, which requires an ion isolation resolving power of 100 000. Figure 6a shows the fragmentation spectrum of m/z 352.22192 ($[C_{24}H_{32}S_1]^{\bullet+}$) from (+) APPI of Athabascan Canadian bitumen after SWIFT isolation of m/z 352.22192 (16 MB waveform, 48% isolation efficiency) and IRMPD. Two series of fragments are detected: the series that corresponds to the precursor ion ($C_cH_hS_1^{\bullet+}$) and the loss of $H^{\bullet}$ ($C_cH_{h-1}S_1^{+}$). A pattern of consecutive C_1H_2 loss is observed, which corresponds to the loss of an alkyl chain from the core structure. Figure 6b shows an isoabundance-contoured plot of

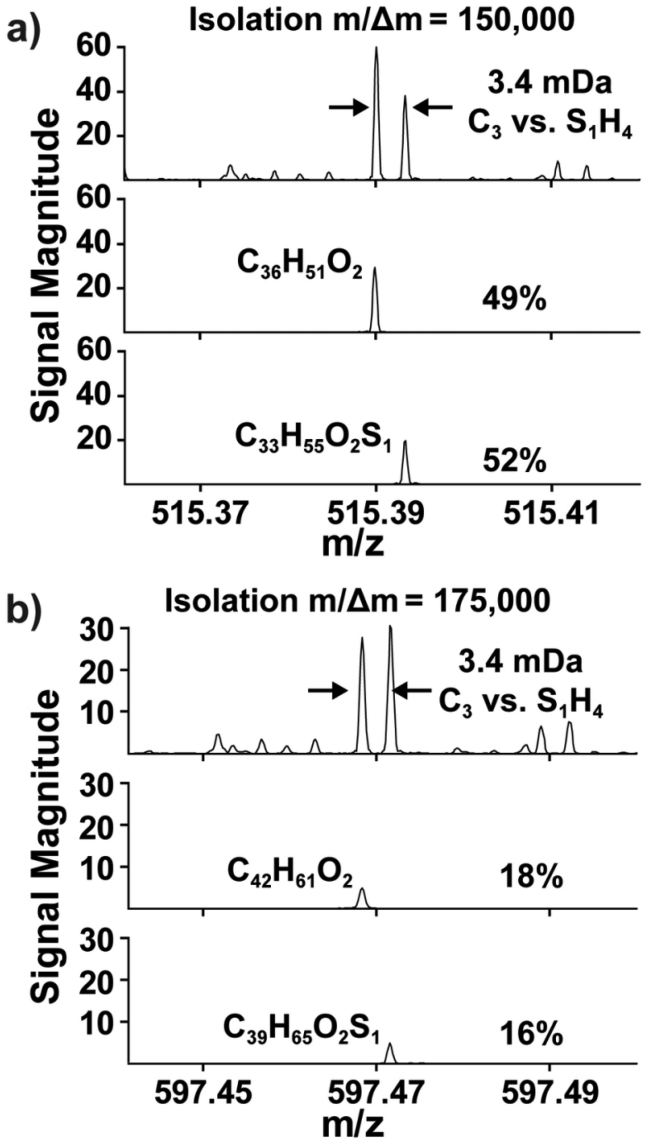

Figure 5. Ultrahigh ion isolation resolving power of ions that differ in mass by 3.4 mDa from (−) ESI of Athabascan Canadian bitumen. (a) 16 MB SWIFT was used to isolate two ions that require an isolation resolving power of 150 000 at m/z 515, with ~50% isolation efficiency. (b) 32 MB SWIFT was used to isolate two ions that require an isolation resolving power of 175 000 at m/z 597, with ~17% isolation efficiency.

double bond equivalents (DBE; the number of rings and/or double bonds) versus number of carbons for members of the $S_1^{\bullet+}$ class, as assigned from the spectrum in Figure 6a. The red cross denotes the precursor ion. The ion loses C_1H_2 units but without the loss of DBE, indicative of an alkyl chain attached to a condensed core. The absence of the first two C_1H_2 losses is attributed to the low signal-to-noise of the spectrum. The increase in DBE at lower carbon number is indicative of H_2 loss. The fragment ion detected at m/z 184.03412 has a molecular formula of $[C_{12}H_8S_1]^{\bullet+}$, which is consistent with the proposed structure of dibenzothiophene shown in Figure 6b. Thus, the structure of the ion at m/z 352.22192 is tentatively identified as a dibenzothiophene core with an additional 12 carbons attached as alkyl chains.

High-resolution SWIFT isolations enable the characterization of components beyond the assignment of molecular

https://dx.doi.org/10.1021/acs.analchem.9b04954
Anal. Chem. 2020, 92, 3213−3219

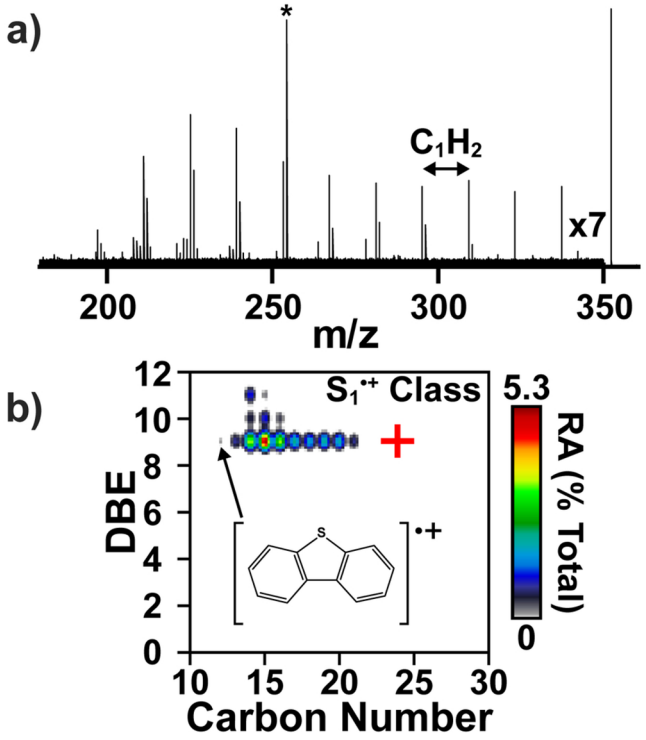

Figure 6. High-resolution ion isolation of a single, unique m/z from (+) APPI of Athabascan Canadian bitumen. (a) IRMPD fragmentation mass spectrum. A mass spacing corresponding to the loss of C_1H_2 units is observed across the m/z range, which indicates loss of alkyl chain units. The spectrum is an average of 60 time-domain transients. The asterisk indicates electronic noise. (b) Isoabundance-contoured plots of DBE versus number of carbons for members of the $S1^{\bullet+}$ class. The red cross indicates the precursor ion. Loss of alkyl chain units is observed as a constant DBE but decreasing carbon number. The inset structure is the predicted dibenzothiophene core, $[C_{12}H_8S_1]^{\bullet+}$, which would correspond to the ion detected at m/z 184.03412, indicated by the black arrow.

formula, albeit structural isomers cannot be separated by this method. This represents an order of magnitude improvement in achieved isolation resolving power required to isolate a single unique m/z value, likely a single elemental composition, from a complex organic mixture.[28]

CONCLUSIONS

SWIFT isolation by 21 T FTICR offers significant advantages for precursor ion isolations from complex samples. Fast and efficient SWIFT waveforms enable high selectivity top-down proteoform characterization from bulk histone LC-MS experiments. SWIFT isolation becomes more challenging as the peak density of the spectrum increases. Therefore, waveforms of increasing duration must be applied to cleanly isolate the desired ions of interest, at the cost of throughput and reduced signal magnitude of isolated species. Nonetheless, we were able to isolate single m/z ions from a complex mixture that differ by 0.0034 Da at m/z 597. We anticipate improved SWIFT isolation efficiency by lowering the pressure in the ICR cell region and by careful tuning of the excitation circuitry. The minimum achievable isolation width for complex mixture analysis has been reduced to 0.0034 m/z (from ~0.03 m/z in previous studies). This now enables the investigation of single m/z values from complex mixtures by tandem MS for structural determination of molecules from dissolved organic matter, petroleum, petroleum derived mixtures, and other small molecules.

ASSOCIATED CONTENT

Supporting Information

The Supporting Information is available free of charge at https://pubs.acs.org/doi/10.1021/acs.analchem.9b04954.

Time domain and frequency domain SWIFT waveforms, two additional examples of histone characterization by SWIFT UVPD, broadband (-) ESI FT-ICR MS of Athabascan Canadian bitumen (PDF)

AUTHOR INFORMATION

Corresponding Author

Christopher L. Hendrickson − *National High Magnetic Field Laboratory and Department of Chemistry and Biochemistry, Florida State University, Tallahassee, Florida 32310, United States*; Phone: (850)-644-0711; Email: hendrick@magnet.fsu.edu; Fax: (850)-644-1366

Authors

Donald F. Smith − *National High Magnetic Field Laboratory, Florida State University, Tallahassee, Florida 32310, United States*; orcid.org/0000-0003-3331-0526

Greg T. Blakney − *National High Magnetic Field Laboratory, Florida State University, Tallahassee, Florida 32310, United States*; orcid.org/0000-0002-4205-9866

Steven C. Beu − *S.C. Beu Consulting, Austin, Texas 78729, United States*

Lissa C. Anderson − *National High Magnetic Field Laboratory, Florida State University, Tallahassee, Florida 32310, United States*

Chad R. Weisbrod − *National High Magnetic Field Laboratory, Florida State University, Tallahassee, Florida 32310, United States*

Complete contact information is available at: https://pubs.acs.org/10.1021/acs.analchem.9b04954

Notes

The authors declare no competing financial interest.

ACKNOWLEDGMENTS

A portion of this work was performed at the National High Magnetic Field Laboratory ICR User Facility, which is supported by the National Science Foundation Division of Chemistry through Grants DMR-1157490 and DMR-1644779 and the State of Florida. We thank Professor Michelle Arbeitman for the histone samples. The 21 T FTICR mass spectrometer is available free of charge to all qualified users as part of the NSF High Field FTICR Mass Spectrometry User Facility.

REFERENCES

(1) Cui, W.; Rohrs, H. W.; Gross, M. L. *Analyst* **2011**, *136*, 3854.

(2) Smith, L. M.; Kelleher, N. L.; Linial, M.; Goodlett, D.; Langridge-Smith, P.; Ah Goo, Y.; Safford, G.; Bonilla, L.; Kruppa, G.; Zubarev, R.; Rontree, J.; Chamot-Rooke, J.; Garavelli, J.; Heck, A.; Loo, J.; Penque, D.; Hornshaw, M.; Hendrickson, C.; Pasa-Tolic, L.; Borchers, C.; Chan, D.; Young, N.; Agar, J.; Masselon, C.; Gross, M.; McLafferty, F.; Tsybin, Y.; Ge, Y.; Sanders, I.; Langridge, J.; Whitelegge, J.; Marshall, A. *Nat. Methods.* **2013**, *10*, 186.

(3) Chen, B.; Brown, K. A.; Lin, Z.; Ge, Y. *Anal. Chem.* **2018**, *90*, 110−127.

(4) Marshall, A. G.; Rodgers, R. P. *Proc. Natl. Acad. Sci. U. S. A.* **2008**, *105*, 18090−18095.
(5) Cho, Y.; Ahmed, A.; Islam, A.; Kim, S. *Mass Spectrom. Rev.* **2015**, *34*, 248−263.
(6) Smith, D. F.; Podgorski, D. C.; Rodgers, R. P.; Blakney, G. T.; Hendrickson, C. L. *Anal. Chem.* **2018**, *90*, 2041−2047.
(7) Houel, S.; Abernathy, R.; Renganathan, K.; Meyer-Arendt, K.; Ahn, N. G.; Old, W. M. *J. Proteome Res.* **2010**, *9*, 4152−4160.
(8) Heck, A. J. R.; de Koning, L. J.; Pinkse, F. A.; Nibbering, N. M. M. *Rapid Commun. Mass Spectrom.* **1991**, *5*, 406−414.
(9) de Koning, L. J.; Nibbering, N. M. M.; van Orden, S. L.; Laukien, F. H. *Int. J. Mass Spectrom. Ion Processes* **1997**, *165*−*166*, 209−219.
(10) Marshall, A. G.; Lin Wang, T.; Lebatuan Ricca, T. *Chem. Phys. Lett.* **1984**, *105*, 233−236.
(11) Marshall, A. G.; Wang, T. C. L.; Ricca, T. L. *J. Am. Chem. Soc.* **1985**, *107*, 7893−7897.
(12) Guan, S.; Marshall, A. G. *Int. J. Mass Spectrom. Ion Processes* **1996**, *157*, 5−37.
(13) Heck, A. J. R.; Derrick, P. J. *Eur. Mass Spectrom.* **1998**, *4*, 181−188.
(14) O'Connor, P. B.; McLafferty, F. W. *J. Am. Soc. Mass Spectrom.* **1995**, *6*, 533−535.
(15) Julian, R. K.; Cooks, R. G. *Anal. Chem.* **1993**, *65*, 1827−1833.
(16) Soni, M. H.; Cooks, R. G. *Anal. Chem.* **1994**, *66*, 2488−2496.
(17) Hu, Q.; Cooks, R. G.; Noll, R. J. *J. Am. Soc. Mass Spectrom.* **2007**, *18*, 980−983.
(18) Fischer, P.; Knauer, S.; Marx, G.; Schweikhard, L. *Rev. Sci. Instrum.* **2018**, *89*, 015114.
(19) Dickel, T.; Plaß, W. R.; Lippert, W.; Lang, J.; Yavor, M. I.; Geissel, H.; Scheidenberger, C. *J. Am. Soc. Mass Spectrom.* **2017**, *28*, 1079−1090.
(20) Johnson, J. T.; Carrick, I. J.; Eakins, G. S.; McLuckey, S. A. *Anal. Chem.* **2019**, *91*, 8789−8794.
(21) Tran, J. C.; Zamdborg, L.; Ahlf, D. R.; Lee, J. E.; Catherman, A. D.; Durbin, K. R.; Tipton, J. D.; Vellaichamy, A.; Kellie, J. F.; Li, M.; Wu, C.; Sweet, S. M. M.; Early, B. P.; Siuti, N.; LeDuc, R. D.; Compton, P. D.; Thomas, P. M.; Kelleher, N. L. *Nature* **2011**, *480*, 254.
(22) Anderson, L. C.; Dehart, C. J.; Kaiser, N. K.; Fellers, R. T.; Smith, D. F.; Greer, J. B.; Leduc, R. D.; Blakney, G. T.; Thomas, P. M.; Kelleher, N. L.; Hendrickson, C. L. *J. Proteome Res.* **2017**, *16*, 1087−1096.
(23) Fornelli, L.; Durbin, K. R.; Fellers, R. T.; Early, B. P.; Greer, J. B.; LeDuc, R. D.; Compton, P. D.; Kelleher, N. L. *J. Proteome Res.* **2017**, *16*, 609−618.
(24) Zheng, Y.; Fornelli, L.; Compton, P. D.; Sharma, S.; Canterbury, J.; Mullen, C.; Zabrouskov, V.; Fellers, R. T.; Thomas, P. M.; Licht, J. D.; Senko, M. W.; Kelleher, N. L. *Mol. Cell. Proteomics* **2016**, *15*, 776−790.
(25) Guan, S.; Burlingame, A. L. *J. Am. Soc. Mass Spectrom.* **2010**, *21*, 455−459.
(26) Podgorski, D. C.; Corilo, Y. E.; Nyadong, L.; Lobodin, V. V.; Bythell, B. J.; Robbins, W. K.; McKenna, A. M.; Marshall, A. G.; Rodgers, R. P. *Energy Fuels* **2013**, *27*, 1268−1276.
(27) Wittrig, A. M.; Fredriksen, T. R.; Qian, K.; Clingenpeel, A. C.; Harper, M. R. *Energy Fuels* **2017**, *31*, 13338−13344.
(28) Witt, M.; Fuchser, J.; Koch, B. P. *Anal. Chem.* **2009**, *81*, 2688−2694.
(29) Hendrickson, C. L.; Quinn, J. P.; Kaiser, N. K.; Smith, D. F.; Blakney, G. T.; Chen, T.; Marshall, A. G.; Weisbrod, C. R.; Beu, S. C. *J. Am. Soc. Mass Spectrom.* **2015**, *26*, 1626−1632.
(30) Nikolaev, E. N.; Boldin, I. A.; Jertz, R.; Baykut, G. *J. Am. Soc. Mass Spectrom.* **2011**, *22*, 1125−1133.
(31) Hendrickson, C. L.; Beu, S. C.; Blakney, G. T.; Kaiser, N. K.; McIntosh, D. G.; Quinn, J. P.; Marshall, A. G. Optimized Cell Geometry for Fourier Transform Ion Cyclotron Resonance Mass Spectrometry. *Proceedings of the 57th ASMS Conference on Mass Spectrometry & Allied Topics*, Philadelphia, PA, May 31−June 4, 2009.
(32) Chen, T.; Beu, S. C.; Kaiser, N. K.; Hendrickson, C. L. *Rev. Sci. Instrum.* **2014**, *85*, 066107.
(33) Kaiser, N. K.; Chen, T.; Quinn, J. P.; Beu, S. C.; Hendrickson, C. L.; Marshall, A. G. Experimental Evaluation of Current State of the Art FT-ICR Cell Technology. *Proceedings of the 61st ASMS Conference on Mass Spectrometry & Allied Topics*, Minneapolis, MN, June 9−13, 2013.
(34) Blakney, G. T.; Hendrickson, C. L.; Marshall, A. G. *Int. J. Mass Spectrom.* **2011**, *306*, 246−252.
(35) Guan, S.; McIver, R. T. *J. Chem. Phys.* **1990**, *92*, 5841−5846.
(36) Guan, S. *J. Chem. Phys.* **1989**, *91*, 775−777.
(37) Schweikhard, L.; Marshall, A. G. *J. Am. Soc. Mass Spectrom.* **1993**, *4*, 433−452.
(38) Corilo, Y. E. *PetroOrg. Software*; Florida State University, Omics LLC: Tallahassee, FL, 2014.
(39) Horn, D. M.; Zubarev, R. A.; McLafferty, F. W. *J. Am. Soc. Mass Spectrom.* **2000**, *11*, 320−332.
(40) Fellers, R. T.; Greer, J. B.; Early, B. P.; Yu, X.; LeDuc, R. D.; Kelleher, N. L.; Thomas, P. M. *Proteomics* **2015**, *15*, 1235−1238.

https://dx.doi.org/10.1021/acs.analchem.9b04954
Anal. Chem. 2020, 92, 3213−3219